Hindawi Publishing Corporation
Journal of Nanomaterials
Volume 2012, Article ID 760872, 9 pages
doi:10.1155/2012/760872

Research Article

Polyol-Mediated Synthesis of Zinc Oxide Nanorods and Nanocomposites with Poly(methyl methacrylate)

Alojz Anžlovar,[1,2] Zorica Crnjak Orel,[1,2] Ksenija Kogej,[3] and Majda Žigon[1,2]

[1] *Center of Excellence for Polymer Materials and Technologies, Tehnološki Park 24, 1000 Ljubljana, Slovenia*
[2] *Laboratory for Polymer Chemistry and Technology, National Institute of Chemistry, Hajdrihova 19, 1000 Ljubljana, Slovenia*
[3] *Chair of Physical Chemistry, Faculty of Chemistry and Chemical Technology, University of Ljubljana, Aškerčeva 5, 1000 Ljubljana, Slovenia*

Correspondence should be addressed to Alojz Anžlovar, alojz.anzlovar@ki.si

Received 22 January 2012; Revised 7 April 2012; Accepted 10 April 2012

Academic Editor: Sevan P. Davtyan

ZnO nanorods (length 30–150 nm) were synthesized in di(ethylene glycol) using $Zn(CH_3COO)_2$ as a precursor and *para*-toluene sulphonic acid, p-TSA, as an end-capping agent. Increasing the concentration of p-TSA above 0.1 M causes the reduction of the ZnO length. Nanocomposites with poly(methyl methacrylate) were prepared using unmodified nanorods. They enhanced the UV absorption of nanocomposites (~98%) at low ZnO concentrations (0.05–0.1 wt.%), while visible light transparency was high. At concentrations of 1 wt.% and above, nanorods enhanced the thermal stability of nanocomposites. At low concentrations (0.05–0.1 wt.%), they increased the storage modulus of material and shifted T_g towards higher temperatures as shown by dynamic mechanical analysis, DMA, while at higher concentrations (1.0 wt.%) this effect was deteriorated. DMA also showed that spherical ZnO particles have a more pronounced effect on the storage modulus and T_g than nanorods.

1. Introduction

Nanostructured materials constitute one of the most propulsive fields of materials, science and have received great attention due to their potential application [1, 2] in various fields such as electronics [3], microelectronics [4–6], sensors [7], photovoltaics [8, 9], electro-optical devices [10–12], and catalysis [13]. Zinc oxide (ZnO) is an inorganic material with a large direct band gap (3.34 eV), high exciton binding energy (60 meV), high isoelectric point (9.5), and fast electron transfer kinetics as well as having a unique combination of properties [14, 15]. All these features suggest the synthesis of special ZnO nanostructures and how to use these materials in novel unexplored applications. Nano ZnO can be synthesized in many forms: rods, wires, whiskers, belts, bipods, tetrapods, tubes, flowers, propellers, bridges, and cages [16–18]. A special field of nanomaterials is represented by extended and oriented nanostructures which are desirable for many applications [19].

One-dimensional ZnO nanostructures have been synthesized by many preparation techniques such as thermal evaporation, hydrothermal synthesis, metal organic chemical vapor deposition, spray pyrolysis, ion beam-assisted deposition, laser ablation, sputter deposition, template-assisted growth, chemical vapor deposition, sol-gel process, and solvothermal synthesis [20–22]. ZnO nanorods have been synthesized also by solvothermal reaction in various alcohols [23, 24].

A special type of solvothermal synthesis of ZnO is the polyol procedure which uses various diols as a reaction medium [25, 26]. Besides acting as a reaction medium polyol also serves as a stabilizing agent and it reduces the particle growth [27–29]. The advantage of the polyol procedure is that it produces particles with an organophilic surface layer which needs no additional surface modification for the application in nanocomposites [30]. Combining the organic polymers with inorganic particles, fillers can result in materials with enhanced mechanical and other properties [31]. By reducing the size of filler the interface between the filler particles and the polymer matrix is substantially increased and therefore their impact on the properties of the composite is significantly enhanced [32, 33]. Many polymer materials undergo chemical degradation when exposed to sunlight. Due to the thinner ozone layer and higher intensity of UV

light, their degradation is becoming more intense and consequently their UV stabilization is of increased importance. Poly(methyl methacrylate), PMMA, is an amorphous thermoplastic material with exceptional optical properties. Due to favorable mechanical and processing properties, it replaces inorganic glass in many applications [30]. Despite intense research efforts, the development of a simple and effective method of preparation of homogeneous nanocomposites with PMMA matrix on both the laboratory and on the industrial scale is still a challenge. By combining the PMMA matrix and nano ZnO, transparent materials with high UV absorption and improved thermal stability can be prepared.

In the present work we report on the synthesis of ZnO nanorods with organophilic surface at high concentration of the precursor (1 M) by the polyol method, using di(ethylene glycol), DEG, as a medium and *p*-toluene sulphonic acid, p-TSA, as an end capping agent. The primary aim of our work was to demonstrate that homogeneous transparent PMMA/ZnO nanocomposites using unmodified ZnO nanorods, synthesized by the polyol method, can be prepared with potential application as UV stabilized PMMA materials with enhanced properties. UV stabilization using ZnO nanoparticles as UV absorbers represents an alternative to conventional UV stabilizers. The secondary aim was to determine the difference between the impacts of spherical ZnO particles and ZnO nanorods on the properties of PMMA/ZnO nanocomposites.

2. Experimental

2.1. Materials. The materials used are di(ethylene glycol), DEG (Merck, 99%, for synthesis); Zinc(II) acetate monohydrate, $Zn(Ac)_2$ (Sigma-Aldrich, 99%, ACS reagent); *p*-toluenesulfonic acid monohydrate, p-TSA (Sigma-Aldrich, 98.5%, ACS reagent); methyl methacrylate, MMA (technical); *1,1-Azobis*(1-cyclohexanecarbonitrile), AICN (Aldrich, 98%); and ethanol (technical).

2.2. Synthesis of ZnO Nanorods. Zinc(II) acetate (1.0 M), p-TSA (0.1 M), and deionised water (2 mole/1 mole Zn) were mixed with 60 mL of DEG and sonicated for 10 min. The mixture was transferred into a 250 mL glass reactor equipped with a mixer, condenser, and digital thermometer. The temperature and color changes of the reaction medium were monitored over time. The temperature was raised over about 10 min to 190°C and kept constant for 50 min with constant stirring. Between 90°C and 120°C $Zn(Ac)_2$ dissolved in the DEG, after 20 to 30 minutes at 190°C the solution became white, and after 60 min a white suspension of ZnO was obtained. The suspension was left overnight and centrifuged (8000 rpm, 20 min). The ZnO was washed twice with ethanol and centrifuged (8000 rpm, 20 min.). The obtained ZnO powder was left to air dry. Spherical ZnO nanoparticles were synthesized by the same procedure in ethylene glycol (size 20–40 nm) and in 1,2-propane diol (size 30–50 nm) [34].

2.3. Synthesis of ZnO/PMMA Nanocomposites. Nanocomposites of the synthesized ZnO nanorods and PMMA matrix were prepared by the radical chain polymerization of MMA monomer in bulk in three variations: radical polymerization between glass plates starting directly from the ZnO dispersion in monomer (MMA) (procedure A), polymerization between glass plates starting from the previously prepared dispersion of ZnO in prepolymer (procedure B), and polymerization between two glass plates starting from ZnO dispersion in prepolymer which was polymerized during constant sonication (procedure C). The detailed description of all three procedures is given in the previous publication [34]. The nanocomposite plate thickness using procedure A was 1.5 mm, while procedures B and C gave nanocomposite plates with a thickness of 3.5 mm.

2.4. Characterization Methods. The morphology of the synthesized ZnO nanorods was studied by SEM (Zeiss Supra 35 VP, acceleration voltage −3.37 or 5.0 kV, working distance, 3–6 mm, gold-sputtered samples) and HR TEM electron microscopy (JEM 2000FX microscope, JEOL, acceleration voltage −200 kV). For HR TEM microscopy, ZnO nanorods were dispersed in an organic solvent. A drop of dispersion was placed on a Cu grid and left to evaporate the solvent. The nanocomposite materials were studied by STEM microscopy (Supra 35 VP, Zeiss, acceleration voltage −20.0 kV, working distance −4.5–5 mm, STEM detector, ultramicrotomed sections). Nanocomposites were sectioned on the ultramicrotome (Leica Ultracut, Leica, thickness 80–250 nm).

The sizes of ZnO nanorods and their aggregates in MMA were measured by dynamic light scattering (3D-DLS-SLS spectrometer, LS Instruments equipped with 20 mV He-Ne laser—Uniphase JDL 1145, P, wavelength 632.8 nm). Scattering was measured at an angle of 90°. Samples in scattering cells were immersed in a thermostated bath at 20°C, and ten measurements of 60 s were recorded for each sample and averaged afterwards. The translational diffusion coefficient, D, was determined while the hydrodynamic radius, R_h, was calculated from D using the Stokes-Einstein equation (viscosity of MMA, $\eta = 0.6$ cP at 20°C).

UV-Vis spectra of nanocomposites were measured on an Agilent 8453 UV-Vis spectrometer, Agilent Technologies, (spectral range 290–380 nm, sample width 12 mm, thickness 1.6 and 3.5 mm).

The chemical composition of ZnO nanorods was studied by FTIR spectroscopy using an FTIR spectrometer (Spectrum One, Perkin Elmer, spectral range 400–4000 cm^{-1}, spectral resolution 4 cm^{-1}, transmittance mode, KBr pellets).

Thermal properties of PMMA/ZnO nanorod composites were studied by TGA (STA 409, Netsch, temperature range 50–600°C, heating rate 1°C/min, air flux of 100 mL/min, sample quantity ~50 mg).

Crystalline fractions of nano-ZnO were characterized by XRD diffraction (D-5000 diffractometer, Siemens, Cu anode as the X-ray source, 25°C, 2Θ range 2–90°, step 0.04°, step time 1 s). Crystallite sizes were calculated using the Scherrer formula.

DMA measurements were performed on DMA Q800, Thermal Analysis, using a single cantilever clamp (temperature range 30–150°C, heating rate 5°C/min, amplitude 15 μm, frequency 10 Hz).

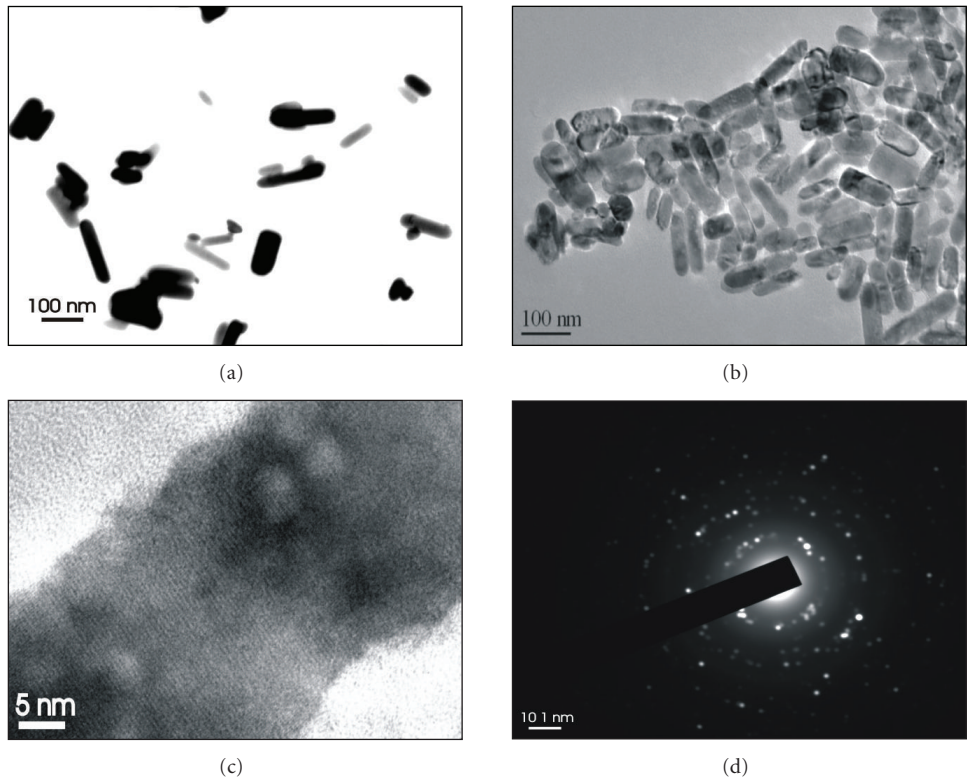

Figure 1: (a) STEM micrograph, (b) and (c) HR-TEM micrographs of ZnO nanorods, and (d) electron diffraction pattern of ZnO nanorods.

3. Results and Discussion

ZnO nanorods were synthesized by the hydrolysis of Zn(II) acetate in DEG with p-TSA as the end-capping agent, while in other diols predominantly spherical ZnO particles were produced. STEM and HR TEM micrographs (Figures 1(a) and 1(b)) show ZnO particles in the form of nanorods (diameter 10–50 nm, length 30–150 nm) with narrow particle size distribution. The HR TEM micrograph in Figure 1(c) shows characteristic crystallite fringes confirming that nanorods are highly crystalline.

The XRD diffractogram (Figure 2(a)(A)) shows characteristic ZnO diffraction maxima at 2Θ values of 31.8, 34.5, 36.2, 47.6, 56.6, 62.9, 66.4, 67.9, 69.1, 72.6, and 76.9 [35]. Calculated crystallite size using the Scherrer equation [36] is 45 nm. Compared to the XRD diffractogram of spherical ZnO nanoparticles (Figure 2(a)(B)) it shows higher intensity of (002) peak, indicating the preferential growth of wurtzite rods along (002) direction (c-axis) [8, 18, 24, 37, 38]. The preferential growth in one direction is the consequence of the growth rate difference in various directions of the ZnO crystal. It is reported that during hydrothermal synthesis the relative growth of (0001) face is higher than that of other ones, leading to the formation of extended prismatic hexagonal ZnO crystals [39]. Nanorod growth is, as reported, caused by the adsorption of DEG molecules to the nonpolar faces of the crystal, while highly polar (0001) faces at both ends are able to develop and grow faster resulting in the formation of ZnO nanorods [40]. This explains why ZnO nanorods are formed only in DEG, while in other diols ZnO with regular morphology is formed [34]. The crystallinity of ZnO nanorods was additionally confirmed by HR TEM microscopy where characteristic fringes of crystallites were observed (Figure 1(c)). The electron diffraction pattern (Figure 1(d)) confirms that synthesized ZnO nanorods are polycrystalline. By increasing the concentration of p-TSA from 0.1 to 0.4 M the length of ZnO nanorods was reduced, indicating its important role in the mechanism of ZnO particle formation (Table 1).

The IR spectrum of ZnO usually shows a characteristic absorption band between 420 and 510 cm^{-1} due to two transverse optical stretching modes of ZnO [41]. In the case of ZnO nanorods this maximum is split into two maxima, one at 507 and the second one at 423 cm^{-1} (Figure 2(b)(A)), while spherical ZnO nanoparticles show only one maximum at 471 cm^{-1} (Figure 2(b)(B)) [21, 42, 43]. These two absorption peaks correlate with the bulk TO-phonon frequency and the LO-phonon frequency [44]. Additional absorption bands at 1590, 1415, and 1340 cm^{-1} were ascribed to organic impurities originating from reaction intermediates, which can be identified as Zn hydroxo acetate complex [45] or tetra nuclear oxo zinc acetate cluster ($Zn_4O(CH_3COO)_6$) [34, 46, 47], while the one at 3435 cm^{-1} was assigned to the OH groups on the surface of ZnO.

The combination of PMMA matrix and ZnO nanoparticles gives optically transparent materials with high UV absorption [16]. Such materials have high potential in various outdoor applications with high UV light loads.

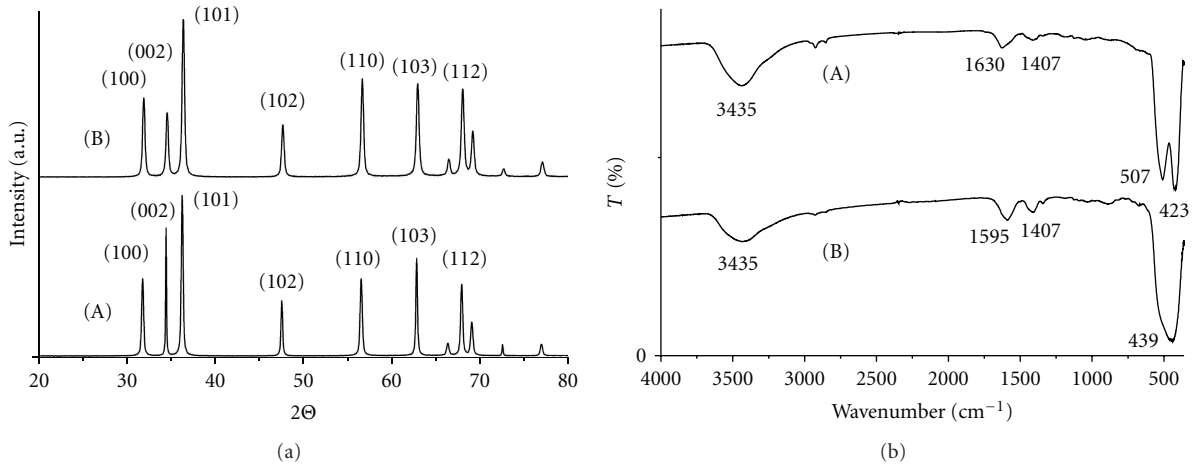

Figure 2: (a) XRD diffractograms and (b) FTIR spectra of (A) ZnO nanorods and (B) ZnO nanoparticles.

Table 1: The length of ZnO nanowires in correlation with the p-TSA concentration.

Designation of the sample	Concentration of p-TSA (mol/L)	Length of ZnO nanorods (nm)
ZnO-1	0.05	50–180
ZnO-2	0.1	50–150
ZnO-3	0.2	30–100
ZnO-4	0.4	20–70

For the preparation of PMMA/ZnO nanocomposites, ZnO nanorods were first dispersed in MMA which was subsequently polymerized by free-radical chain polymerization of MMA in situ between glass plates starting (a) directly from the ZnO dispersion in MMA (procedure A), (b) from previously prepared dispersion of ZnO in prepolymer (procedure B), and (c) the same as in procedure B only with constant sonication during the entire polymerization process (procedure C).

The most important parameter in preparing the homogeneous PMMA/ZnO nanocomposites is dispersion stability of ZnO particles in MMA monomer. Dispersion stability, that is, R_h of ZnO nanorods in dependence of time and ZnO concentration (Table 2), was studied by dynamic light scattering, DLS. Comparing R_h after 10 min and after 25 min we observed an increase of R_h indicating a slight aggregation of ZnO nanorods in MMA, but at longer times (45 min) R_h no longer increased, indicating that the dispersion became stable. The stability of ZnO nanorod/MMA dispersion can be explained by the strong interactions between ZnO surface and carbonyl groups of MMA [48].

When MMA is polymerized by the radical chain mechanism, the weight average molar mass, M_w, of PMMA reaches values well above 100 000 g/mol [30] after 45 min of reaction, and this can explain the stability of dispersion of ZnO nanorods in the reaction mixture. It has been reported [49] that at isothermal conditions, at temperatures between 70 and 80°C, bulk radical chain polymerization of MMA reaches gel effect (Tromsdorff effect) in reaction time between 25 and 50 min. Gel effect raises the viscosity of the system in a few minutes to values above 1×10^6 Pa s, and due to the high viscosity of the system ZnO nanorods remain dispersed in the PMMA matrix.

The distribution of ZnO nanorods in the PMMA nanocomposites prepared by procedure A was studied by STEM microscopy of their ultra-microtomed sections. STEM micrographs in Figure 3 show cross sections of PMMA/ZnO nanorod composite containing 1 wt.% of ZnO. The distribution of ZnO nanorods in PMMA is homogeneous with a few agglomerates. The ZnO nanorod structure can be observed only for some of the particles because the nanorods are statistically oriented in the three-dimensional space.

Since ZnO is a highly efficient absorber in the UV region from 32 to 400 nm due to its wide direct band gap of 3.37 eV [50], the addition of nano-ZnO into the PMMA matrix significantly enhances UV absorption and UV resistance of nanocomposite materials [51–53]. Transmittances in the UV-Vis spectral region of PMMA/ZnO nanorod composites, prepared by procedure A, are given in Table 3. ZnO nanorods are extremely efficient UV absorbers since they absorb more than 98% of the incident UV light at concentration of 0.1 wt.% and higher. Transparency for visible light is poor due to the formation of cavities in the PMMA matrix and due to a certain extent of ZnO aggregation.

By modifying the MMA polymerization process (procedure B) the transparency of composites for visible light was improved (Figure 4(A)). The prepolymer procedure significantly reduces the shrinking of PMMA and consequently reduces the cavity formation, thus enhancing the visible transparency of nanocomposites [54]. By reducing the concentration of ZnO, the aggregation of ZnO is substantially reduced and therefore visible transparency has been additionally improved (Figures 4(B) and 4(C), while the absorption in the UV region is reduced only at the ZnO concentration of 0.01 wt.% (Figure 4(C)).

The modification of nanocomposite preparation procedure by the introduction of the sonication through

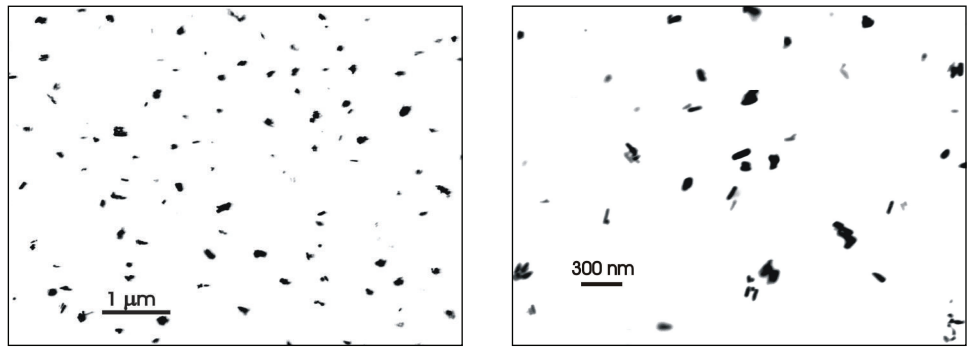

Figure 3: STEM micrographs of ultramicrotomed sections of PMMA/ZnO nanorod composites (1 wt.% of ZnO nanorods) at two magnifications: (a) 50000x and (b) 100000x.

Table 2: Hydrodynamic radii of ZnO nanorods in MMA medium in dependence on the concentration and time.

Sample designation	ZnO concentration (wt.%)	R_h (nm)		
		Time (10 min)	Time (25 min)	Time (45 min)
ZnO (nanorod)/MMA	0.01	102	116	101
ZnO (nanorod)/MMA	0.1	135	198	176

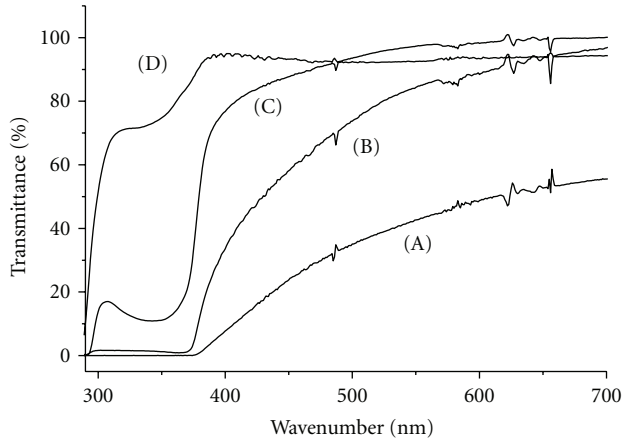

Figure 4: UV-Vis spectra of PMMA/ZnO nanorod composites prepared by procedure B in dependence on ZnO concentration: (A) 0.1 wt.%, (B) 0.05 wt.%, (C) 0.01 wt.%, and (D) PMMA.

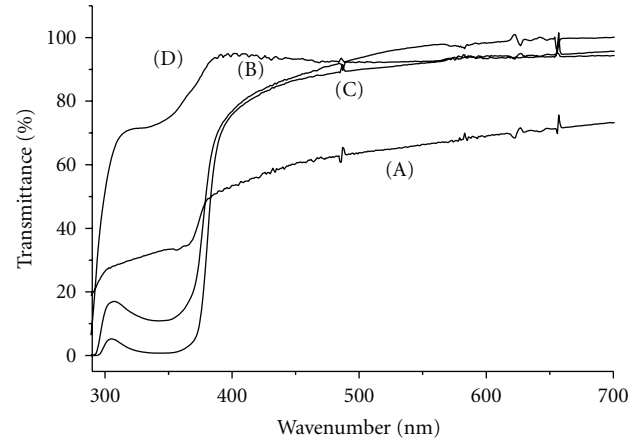

Figure 5: UV-Vis spectra of PMMA/ZnO nanorod composites prepared by different procedures (ZnO concentration = 0.01 wt.%): (A) procedure A, (B) procedure B, (C) procedure C, and (D) PMMA.

the complete prepolymer synthesis (procedure C) additionally reduced ZnO agglomeration enhancing its visible transparency and significantly increasing the absorption in the UV region (Figure 5(C)).

The influence of the addition of ZnO nanorods on the mechanical properties of PMMA nanocomposites was studied by dynamic mechanical analysis, DMA. The storage modulus of nanocomposites is decreasing with temperature due to softening, but it increases with the addition of small amounts of ZnO nanorods (0.01 and 0.1 wt.%), while at higher concentrations (1 wt.%) the reinforcing effect is not intensified (Figure 6(a)). This can be explained by the increased aggregation of ZnO nanorods at higher concentrations, leading to a decrease of the interfacial surface. Similar effects were observed also by other authors [55]. The increase of the storage modulus in the glassy state (up to 75°C) is approximately 25%, while in the intermediate temperature region (from 75°C to 95°C) it is increased by 50 to 100%. Comparison of the storage modulus of PMMA/ZnO nanorods (length 30–150 nm) composites with those of PMMA composites with spherical ZnO nanoparticles (size 20–50 nm, Figure 7(a)) reveals that the latter show a higher increase of the modulus. Therefore ZnO particle size (specific surface-interface) is a more important factor influencing

Table 3: UV light transmittances of PMMA/ZnO nanorod composites in dependence on the UV wavelength and on the ZnO concentration.

Sample designation	Concentration of ZnO [%]	Transmittance at various UV wavelengths (nm) [%]					
		290	300	320	340	360	380
PMMA	—	10.2	51.5	72.1	72.6	79.0	90.8
PMMA/ZnO-1	0.01	19.4	26.5	29.9	32.4	33.9	48.8
PMMA/ZnO-2	0.1	0.16	0.14	0.17	0.042	0.077	0.40
PMMA/ZnO-3	1.0	0.19	0.20	0.31	0.072	0.15	0.047

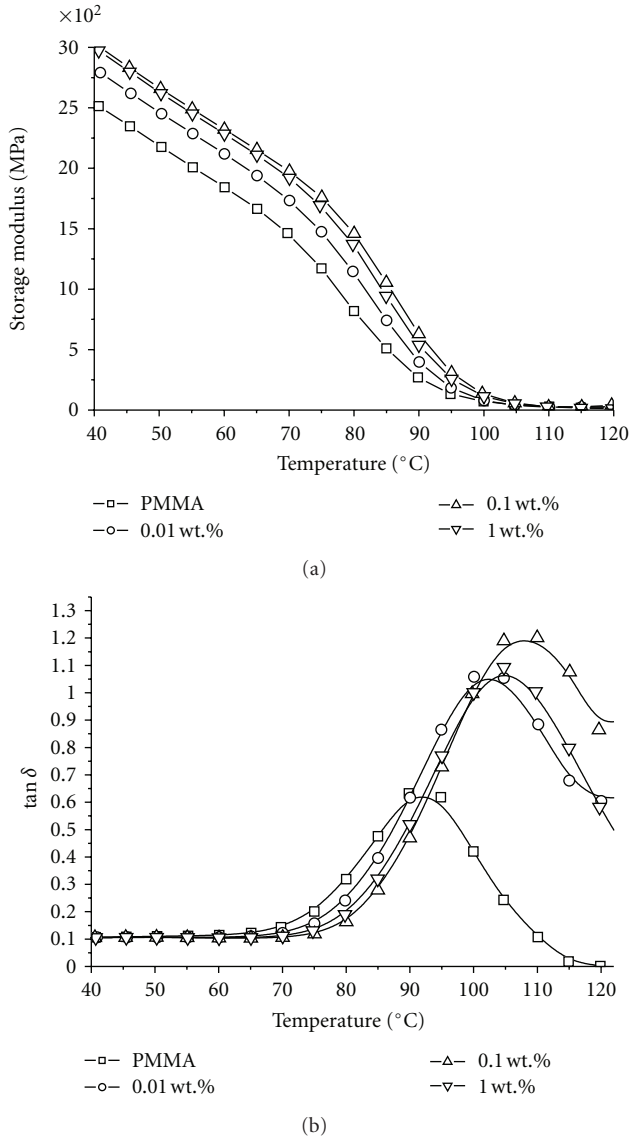

Figure 6: Storage modulus (a) and tan δ (b) of PMMA/ZnO nanorod composites as a function of the ZnO nanorods concentration.

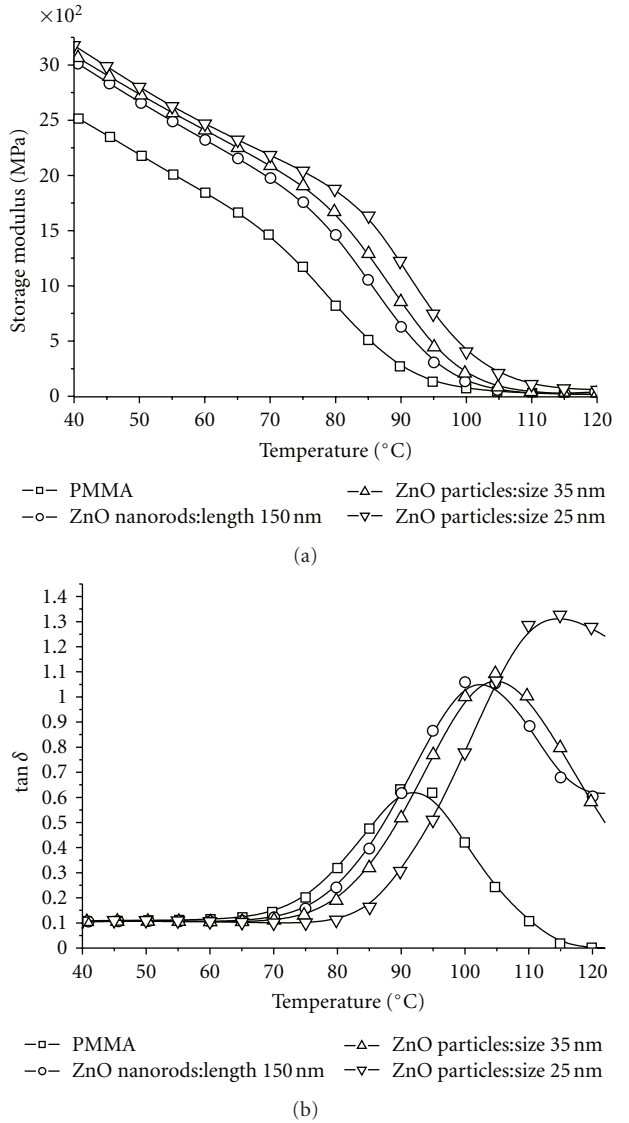

Figure 7: Storage modulus (a) and tan δ (b) of PMMA/ZnO nanorod composites as a function of the ZnO particle size and shape—concentration of ZnO is 0.1 wt.%.

the storage modulus of PMMA/ZnO nanocomposites than is the shape (length) of the particle.

Figure 6(b) shows the dependence of tan δ on the concentration of ZnO nanorods as a function of temperature showing relaxation peaks corresponding to glass transition of the amorphous phase. The dependence reveals that glass transition is shifted to higher temperatures when a low concentration of ZnO nanorods is added (0.01 and 0.1 wt.%), while at higher concentrations no additional shift was observed which is consistent with the results in Figure 6(a). It is interesting that the shift of glass transition temperature to higher temperatures (Figures 6(b) and 7(b))

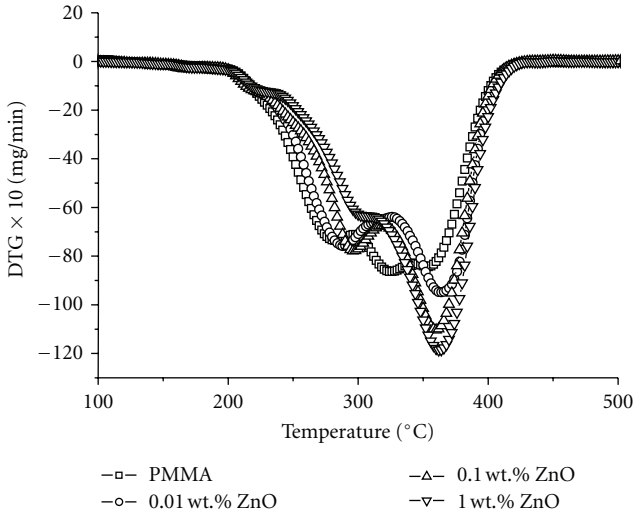

Figure 8: DTG curves of degradation of PMMA/ZnO nanorod composites in dependence on ZnO concentration.

and the increase of storage modulus (Figures 6(a) and 7(a)) both show similar trends. In the temperature region above 85°C, tan δ of these materials is above 0.3 meaning that they are good damping materials [55].

ZnO nanoparticles can substantially enhance the thermal stability of PMMA chains, when MMA is polymerized in their presence [56–58]. DTG decomposition curves of PMMA/ZnO nanorod composites in dependence of ZnO concentration are shown in Figure 8. The DTG curve of pure PMMA (Figure 8) shows three degradation peaks at 270°C (scission of head to head linkages), at 330°C (scission of vinylidene double bonds), and at 370°C (random scission of PMMA chain) [59]. DTG curves of PMMA/ZnO nanorod composites (Figure 8) show less intense peaks of head to head linkage decomposition and of vinylidene double-bond scission at 270 and 330°C, respectively, while the peak of random scission at 370°C becomes much more intense. This indicates that ZnO nanorods thermally stabilize the PMMA matrix in concentration of 1 wt.% and higher. Compared to spherical ZnO nanoparticles their thermal stabilization is less intense. It is interesting to note that thermal stabilization of PMMA is observed only when MMA is polymerized in the presence of nano-ZnO, while nano-ZnO admixed to the PMMA has no influence on the thermal properties of nanocomposite [57]. The absence of a vinylidene double-bond scission peak in DTG curves at ZnO concentrations of 1 wt.% and above suggests that nano-ZnO reduces the double-bond concentration in PMMA chains [57]. The reduced concentration of vinylidene double bonds with increasing ZnO concentration was confirmed by ^{1}H NMR spectroscopy [30].

4. Conclusions

ZnO nanorods with organophilic surface were synthesized by hydrolysis of Zinc(II) acetate in DEG medium with the addition of p-TSA as an end-capping agent. p-TSA reduces the average particle size, increases the ZnO crystallinity, and influences the preferential growth of ZnO in c-axis as shown by the electron microscopy. ZnO nanorods have been synthesized at high concentration of the precursor (1 M), thus allowing their preparation in gram quantities which is beneficial in the preparation of composites.

ZnO nanorods form stable dispersions in MMA for at least 45 min at concentrations of 0.1 wt.% and below. During the radical chain polymerization of MMA, the system reaches gel effect in the reaction time of 20 to 50 min at temperatures between 70 and 80°C. Due to the high viscosity (above 1×10^6 Pa s) of the PMMA/ZnO dispersion, ZnO nanorods remain dispersed in the PMMA matrix.

ZnO nanorods are excellent UV absorbers because they quantitatively absorb UV light in the 290 to 370 nm region at concentrations of 0.1 wt.% of ZnO and above. PMMA plates with high visible light transparency and high UV absorption were prepared using the prepolymer procedure (procedure C). The optimal concentration of ZnO nanorods is between 0.01 and 0.1 wt.% to obtain materials with high absorption of UV light and high transparency for visible light.

DMA analysis of PMMA/ZnO nanorods composites shows that ZnO nanorods increase the storage modulus of nanocomposites and shift the T_g towards higher temperatures at low concentrations (0.01–0.1 wt.%), while at higher concentrations (1.0 wt.%) the reinforcing effect is deteriorated, which was ascribed to the aggregation of ZnO nanorods. Comparing the reinforcing effects of ZnO nanorods and ZnO nanoparticles it was observed that the latter show a more pronounced effect on the storage modulus and T_g than the former, due to their smaller size and larger specific surface.

ZnO nanorods enhance the thermal stability of PMMA at concentrations of 1 wt.% and above. The thermal degradation of PMMA is shifted towards higher temperatures by 20–40°C, which was ascribed to the reduced concentration of vinylidene chain end double bonds as indicated by the changes of DTG curves.

Acknowledgments

The authors acknowledge the financial support from the Ministry of Higher Education, Science and Technology of the Republic of Slovenia through contract no. 3211-10-000057 (Center of Excellence for Polymer Materials and Technologies, PoliMaT). The authors also thank Miroslav Huskić, Ph.D., of the National Institute of Chemistry for the DMA measurements, and Igor Djerdj, Ph.D., of the Rudjer Bošković Institute, Zagreb, Croatia, for HR-TEM microscopy.

References

[1] G. Shen, P. C. Chen, K. Ryu, and C. Zhou, "Devices and chemical sensing applications of metal oxide nanowires," *Journal of Materials Chemistry*, vol. 19, no. 7, pp. 828–839, 2009.

[2] J. P. Cheng, X. B. Zhang, X. Y. Tao, H. M. Lu, Z. Q. Luo, and F. Liu, "Fine-tuning the synthesis of ZnO nanostructures by an alcohol thermal process," *Journal of Physical Chemistry B*, vol. 110, no. 21, pp. 10348–10353, 2006.

[3] C. C. Lin, W. S. Lee, C. C. Sun, and W. H. Whu, "A varistor-polymer composite with nonlinear electrical-thermal switching properties," *Ceramics International*, vol. 34, no. 1, pp. 131–136, 2008.

[4] D. A. Schwartz, N. S. Norberg, Q. P. Nguyen, J. M. Parker, and D. R. Gamelin, "Magnetic quantum dots: synthesis, spectroscopy, and magnetism of Co^{2+}- and Ni^{2+}-doped ZnO nanocrystals," *Journal of the American Chemical Society*, vol. 125, no. 43, pp. 13205–13218, 2003.

[5] W. I. Park, C. H. Lee, J. H. Chae, D. H. Lee, and G. C. Yi, "Ultrafine ZnO nanowire electronic device arrays fabricated by selective metal-organic chemical vapor deposition," *Small*, vol. 5, no. 2, pp. 181–184, 2009.

[6] D. Kabra, M. H. Song, B. Wenger, R. H. Friend, and H. J. Snaith, "High efficiency composite metal oxide-polymer electroluminescent devices: a morphological and material based investigation," *Advanced Materials*, vol. 20, no. 18, pp. 3447–3452, 2008.

[7] C. S. Rout, A. R. Raju, A. Govindaraj, and C. N. R. Rao, "Ethanol and hydrogen sensors based on ZnO nanoparticles and nanowires," *Journal of Nanoscience and Nanotechnology*, vol. 7, no. 6, pp. 1923–1929, 2007.

[8] A. M. Peiró, P. Ravirajan, K. Govender et al., "Hybrid polymer/metal oxide solar cells based on ZnO columnar structures," *Journal of Materials Chemistry*, vol. 16, no. 21, pp. 2088–2096, 2006.

[9] R. Jose, V. Thavasi, and S. Ramakrishna, "Metal oxides for dye-sensitized solar cells," *Journal of the American Ceramic Society*, vol. 92, no. 2, pp. 289–301, 2009.

[10] M. H. Huang, S. Mao, H. Feick et al., "Room-temperature ultraviolet nanowire nanolasers," *Science*, vol. 292, no. 5523, pp. 1897–1899, 2001.

[11] D. P. Liu, G. D. Li, Y. Su, and J. S. Chen, "Highly luminescent ZnO nanocrystals stabilized by ionic-liquid components," *Angewandte Chemie*, vol. 45, no. 44, pp. 7370–7373, 2006.

[12] Y. Hu, Z. Jiang, C. Xu, M. Ting, G. Jun, and W. Tim, "Monodisperse ZnO nanodots: synthesis, charaterization, and optoelectronic properties," *Journal of Physical Chemistry C*, vol. 111, no. 27, pp. 9757–9760, 2007.

[13] A. J. Hoffman, H. Yee, G. Mills, and M. R. Hoffmann, "Photoinitiated polymerization of methyl methacrylate using Q-sized ZnO colloids," *Journal of Physical Chemistry*, vol. 96, no. 13, pp. 5540–5546, 1992.

[14] J. P. Cheng, X. B. Zhang, X. Y. Tao, H. M. Lu, Z. Q. Luo, and F. Liu, "Fine-tuning the synthesis of ZnO nanostructures by an alcohol thermal process," *Journal of Physical Chemistry B*, vol. 110, no. 21, pp. 10348–10353, 2006.

[15] R. Wahab, S. G. Ansari, Y. S. Kim, M. Song, and H. S. Shin, "The role of pH variation on the growth of zinc oxide nanostructures," *Applied Surface Science*, vol. 255, no. 9, pp. 4891–4896, 2009.

[16] J. Zhang, L. Sun, J. Yin, H. Su, C. Liao, and C. Yan, "Control of ZnO morphology via a simple solution route," *Chemistry of Materials*, vol. 14, no. 10, pp. 4172–4177, 2002.

[17] S. K. N. Ayudhya, P. Tonto, O. Mekasuwandumrong, V. Pavarajarn, and P. Praserthdam, "Solvothermal synthesis of ZnO with various aspect ratios using organic solvents," *Crystal Growth and Design*, vol. 6, no. 11, pp. 2446–2450, 2006.

[18] M. Bitenc, P. Podbršček, Z. C. Orel et al., "Correlation between morphology and defect luminescence in precipitated ZnO nanorod powders," *Crystal Growth and Design*, vol. 9, no. 2, pp. 997–1001, 2009.

[19] Z. R. R. Tian, J. A. Voigt, J. Liu et al., "Complex and oriented ZnO nanostructures," *Nature Materials*, vol. 2, no. 12, pp. 821–826, 2003.

[20] Y. W. Heo, D. P. Norton, L. C. Tien et al., "ZnO nanowire growth and devices," *Materials Science and Engineering R*, vol. 47, no. 1-2, pp. 1–47, 2004.

[21] H. Kleinwechter, C. Janzen, J. Knipping, H. Wiggers, and P. Roth, "Formation and properties of ZnO nano-particles from gas phase synthesis processes," *Journal of Materials Science*, vol. 37, no. 20, pp. 4349–4360, 2002.

[22] D.-H. Kuo and B.-J. Chang, "Growth behaviors of ZnO nanorods grown with the Sn-based bilayer catalyst-covered substrates," *Journal of Nanomaterials*, vol. 2011, Article ID 603098, 2011.

[23] P. Tonto, O. Mekasuwandumrong, S. Phatanasri, V. Pavarajarn, and P. Praserthdam, "Preparation of ZnO nanorod by solvothermal reaction of zinc acetate in various alcohols," *Ceramics International*, vol. 34, no. 1, pp. 57–62, 2008.

[24] C. Pacholski, A. Kornowski, and H. Weller, "Self-assembly of ZnO: from nanodots, to nanorods," *Angewandte Chemie International Edition*, vol. 40, no. 7, pp. 1188–1191, 2002.

[25] D. Jezequel, J. Guenot, N. Jouini, and F. Fievet, "Submicrometer zinc oxide particles: elaboration in polyol medium and morphological characteristics," *Journal of Materials Research*, vol. 10, no. 1, pp. 77–83, 1995.

[26] E. W. Seelig, B. Tang, A. Yamilov, H. Cao, and R. P. H. Chang, "Self-assembled 3D photonic crystals from ZnO colloidal spheres," *Materials Chemistry and Physics*, vol. 80, no. 1, pp. 257–263, 2003.

[27] L. Poul, S. Ammar, N. Jouini, F. Fievet, and F. Villain, "Synthesis of inorganic compounds (metal, oxide and hydroxide) in polyol medium: a versatile route related to the sol-gel process," *Journal of Sol-Gel Science and Technology*, vol. 26, no. 1–3, pp. 261–265, 2003.

[28] A. Anžlovar, Z. C. Orel, and M. Žigon, "Copper(I) oxide and metallic copper particles formed in 1,2-propane diol," *Journal of the European Ceramic Society*, vol. 27, no. 2-3, pp. 987–991, 2007.

[29] A. Anžlovar, Z. C. Orel, and M. Žigon, "Morphology and particle size of di(ethylene glycol) mediated metallic copper nanoparticles," *Journal of Nanoscience and Nanotechnology*, vol. 8, no. 7, pp. 3516–3525, 2008.

[30] A. Anžlovar, Z. Crnjak Orel, and M. Žigon, "Poly(methyl methacrylate) composites prepared by in situ polymerization using organophillic nano-to-submicrometer zinc oxide particles," *European Polymer Journal*, vol. 46, no. 6, pp. 1216–1224, 2010.

[31] M. M. Demir, M. Memesa, P. Castignolles, and G. Wegner, "PMMA/zinc oxide nanocomposites prepared by in-situ bulk polymerization," *Macromolecular Rapid Communications*, vol. 27, no. 10, pp. 763–770, 2006.

[32] S. Li, M. S. Toprak, Y. S. Jo, J. Dobson, D. K. Kim, and M. Muhammed, "Bulk synthesis of transparent and homogeneous polymeric hybrid materials with ZnO quantum dots and PMMA," *Advanced Materials*, vol. 19, no. 24, pp. 4347–4352, 2007.

[33] P. Podbršček, G. Dražić, A. Anžlovar, and Z. C. Orel, "The preparation of zinc silicate/ZnO particles and their use as an efficient UV absorber," *Materials Research Bulletin*, vol. 46, no. 11, pp. 2105–2111, 2011.

[34] A. Anžlovar, K. Kogej, Z. Crnjak Orel, and M. Žigon, "Polyol mediated nano size zinc oxide and nanocomposites with

poly(methyl methacrylate)," *Express Polymer Letters*, vol. 5, no. 7, pp. 604–619, 2011.

[35] R. B. Heller, J. McGannon, and A. H. Weber, "Precision determination of the lattice constants of zinc oxide," *Journal of Applied Physics*, vol. 21, no. 12, pp. 1283–1284, 1950.

[36] A. Sinha and B. P. Sharma, "Preparation of copper powder by glycerol process," *Materials Research Bulletin*, vol. 37, no. 3, pp. 407–416, 2002.

[37] S. F. Wang, T. Y. Tseng, Y. R. Wang, C. Y. Wang, and H. C. Lu, "Effect of ZnO seed layers on the solution chemical growth of ZnO nanorod arrays," *Ceramics International*, vol. 35, no. 3, pp. 1255–1260, 2009.

[38] T. Alammar and A. V. Mudring, "Facile ultrasound-assisted synthesis of ZnO nanorods in an ionic liquid," *Materials Letters*, vol. 63, no. 9-10, pp. 732–735, 2009.

[39] W. J. Li, E. W. Shi, W. Z. Zhong, and Z. W. Yin, "Growth mechanism and growth habit of oxide crystals," *Journal of Crystal Growth*, vol. 203, no. 1, pp. 186–196, 1999.

[40] A. Dakhlaoui, M. Jendoubi, L. S. Smiri, A. Kanaev, and N. Jouini, "Synthesis, characterization and optical properties of ZnO nanoparticles with controlled size and morphology," *Journal of Crystal Growth*, vol. 311, no. 16, pp. 3989–3996, 2009.

[41] S. Hayashi, N. Nakamori, and H. Kanamori, "Generalized theory of average dielectric constant and its application to infrared absorption by ZnO small particles," *Journal of the Physical Society of Japan*, vol. 46, no. 1, pp. 176–183, 1979.

[42] L. Wu, Y. Wu, X. Pan, and F. Kong, "Synthesis of ZnO nanorod and the annealing effect on its photoluminescence property," *Optical Materials*, vol. 28, no. 4, pp. 418–422, 2006.

[43] Z. Yang and Q. H. Liu, "The structural and optical properties of ZnO nanorods via citric acid-assisted annealing route," *Journal of Materials Science*, vol. 43, no. 19, pp. 6527–6530, 2008.

[44] Z. Yang, X. Zong, Z. Ye, B. Zhao, Q. Wang, and P. Wang, "The application of complex multiple forklike ZnO nanostructures to rapid and ultrahigh sensitive hydrogen peroxide biosensors," *Biomaterials*, vol. 31, no. 29, pp. 7534–7541, 2010.

[45] L. Znaidi, G. J. A. A. Soler Illia, S. Benyahia, C. Sanchez, and A. V. Kanaev, "Oriented ZnO thin films synthesis by sol-gel process for laser application," *Thin Solid Films*, vol. 428, no. 1-2, pp. 257–262, 2003.

[46] M. K. Johnson, D. B. Powell, and R. D. Cannon, "Vibrational spectra of carboxylato complexes-I. Infrared and Raman spectra of beryllium(II) acetate and formate and of zinc(II) acetate and zinc(II) acetate dihydrate," *Spectrochimica Acta A*, vol. 37, no. 10, pp. 899–904, 1981.

[47] M. K. Johnson, D. B. Powell, and R. D. Cannon, "Vibrational spectra of carboxylato complexes-II. Some oxo-tetranuclear complexes," *Spectrochimica Acta A*, vol. 38, no. 2, pp. 125–131, 1982.

[48] V. D. Koshevar, "The influence of poly(methyl methacrylate) on the stability of zinc oxide dispersions in nonaqueous media of various acidity," *Colloid journal of the Russian Academy of Sciences*, vol. 57, no. 5, pp. 649–652, 1995.

[49] J. S. Sangwai, D. N. Saraf, and S. K. Gupta, "Viscosity of bulk free radical polymerizing systems under near-isothermal and non-isothermal conditions," *Polymer*, vol. 47, no. 9, pp. 3028–3035, 2006.

[50] H. Miyazaki, Y. Teranishi, and T. Ota, "Fabrication of uv-opaque and visible-transparent composite film," *Solar Energy Materials and Solar Cells*, vol. 90, no. 16, pp. 2640–2646, 2006.

[51] G. Kickelbick, "Concepts for the incorporation of inorganic building blocks into organic polymers on a nanoscale," *Progress in Polymer Science*, vol. 28, no. 1, pp. 83–114, 2003.

[52] H. Y. Yu, J. Du, J. S. Gu et al., "Chemical modification on the surface of nano-particles of ZnO and its characterization," *Spectroscopy and Spectral Analysis*, vol. 24, no. 2, pp. 177–179, 2004.

[53] D. Sun, N. Miyatake, and H. J. Sue, "Transparent PMMA/ZnO nanocomposite films based on colloidal ZnO quantum dots," *Nanotechnology*, vol. 18, no. 21, Article ID 215606, 2007.

[54] B. R. Kine, R. W. Novak, and M. Grayson, "Methacrylic polymers," in *Kirk-Othmer Encycopedia of Chemical Technology*, vol. 15, p. 377, Wiley-Interscience, New York, NY, USA, 3rd edition, 1981.

[55] M. Agrawal, S. Gupta, N. E. Zafeiropoulos, U. Oertel, R. Häßler, and M. Stamm, "Nano-level mixing of ZnO into poly(Methyl methacrylate)," *Macromolecular Chemistry and Physics*, vol. 211, no. 17, pp. 1925–1932, 2010.

[56] V. Khrenov, F. Schwager, M. Klapper, M. Koch, and K. Müllen, "Compatibilization of inorganic particles for polymeric nanocomposites. Optimization of the size and the compatibility of ZnO particles," *Polymer Bulletin*, vol. 58, no. 5-6, pp. 799–807, 2007.

[57] M. M. Demir, P. Castignolles, U. Akbey, and G. Wegner, "In-situ bulk polymerization of dilute particle/MMA dispersions," *Macromolecules*, vol. 40, no. 12, pp. 4190–4198, 2007.

[58] Y. Ding, Z. Gui, J. Zhu, Z. Wang, Y. Hu, and L. Song, "Poly(methyl methacrylate)-nanoribbon nanocomposites with high thermal stability and improvement in the glass-transition temperature," *Journal of Materials Research*, vol. 22, no. 12, pp. 3316–3323, 2007.

[59] T. Kashiwagi, A. Inaba, J. E. Brown, K. Hatada, T. Kitayama, and E. Masuda, "Effects of weak linkages on the thermal and oxidative degradation of poly(methyl methacrylates)," *Macromolecules*, vol. 19, no. 8, pp. 2160–2168, 1986.